Screening of classical Casimir forces by electrolytes in semi-infinite geometries

B. Jancovici† and L. Šamaj†‡

† Laboratoire de Physique Théorique, Université de Paris-Sud, Bâtiment 210, 91405 Orsay Cedex, France (Unité Mixte de Recherche no. 8627 - CNRS)
‡ Institute of Physics, Slovak Academy of Sciences, Dúbravská cesta 9, 845 11 Bratislava, Slovakia

E-mail: Bernard.Jancovici@th.u-psud.fr, fyzimaes@savba.sk

Abstract. We study the electrostatic Casimir effect and related phenomena in equilibrium statistical mechanics of classical (non-quantum) charged fluids. The prototype model consists of two identical dielectric slabs in empty space (the pure Casimir effect) or in the presence of an electrolyte between the slabs. In the latter case, it is generally believed that the long-ranged Casimir force due to thermal fluctuations in the slabs is screened by the electrolyte into some residual short-ranged force. The screening mechanism is based on a "separation hypothesis": thermal fluctuations of the electrostatic field in the slabs can be treated separately from the pure image effects of the "inert" slabs on the electrolyte particles. In this paper, by using a phenomenological approach under certain conditions, the separation hypothesis is shown to be valid. The phenomenology is tested on a microscopic model in which the conducting slabs and the electrolyte are modelled by symmetric Coulomb gases of point-like charges with different particle fugacities. The model is solved in the high-temperature Debye-Hückel limit (in two and three dimensions) and at the free fermion point of the Thirring representation of the two-dimensional Coulomb gas. The Debye-Hückel theory of a Coulomb gas between dielectric walls is also solved.

PACS numbers: 05.20.-y, 05.70.-a, 52.25.Kn, 61.20.-p

Keywords: Casimir forces, classical Coulomb gas, charge fluctuations, screening

1. Introduction

Two parallel metallic plates attract one another at zero temperature due to fluctuations of the quantum electromagnetic field in vacuum. This is the well-known Casimir effect; for a nice introduction see reference [1], for an exhausting review see [2]. The extension of Casimir's result to arbitrary temperatures and to general dielectric plates was made by Lifshitz et al. [3], with a subsequent treatment of delicate points by Schwinger et al. [4]. The Casimir force between two disconnected conductor objects of different shapes, like a rectilinear wall and a sphere, is also treatable [1] by using a method due to Derjaguin. The general form of the Casimir free energy for ideal-conductor walls of arbitrary smooth shapes was derived by Balian and Duplantier [5] using multiple scattering expansions (for a review, see [6]). In the classical (or high-temperature) limit defined by the validity of the equipartitioning energy law, the Casimir forces between *disconnected* boundaries become purely entropic [7], and as such depend only on the geometry of the boundaries. For accurate experimental measurements of the Casimir effect see [8].

There is a permanent interest in the Casimir effect and related phenomena in equilibrium statistical mechanics of classical charged fluids, i.e. models of non-quantum charged particles which do not incorporate the magnetic part of the Lorentz force due to charge currents. Although such purely electrostatic models ignore the magnetic degree of freedom (whose effect has the same magnitude as that of the Coulomb force in the case of conducting walls), they can be used in more complex experimental situations to reveal microscopic mechanisms behind macroscopic electrostatics. These classical electrostatic forces are also called van der Waals forces. The statistical models confined by walls can be divided, in general, into two sets: the semi-infinite systems, in which at least one of the spatial coordinates is unconstrained by the walls, and the fully-finite systems. The applied methods and observed phenomena usually depend on this classification. Here, we shall restrict ourselves to the semi-infinite confining geometries, namely the polarizable interface (figure 1) and the two-slab geometry (figure 2). The fully-finite geometries will be treated in a subsequent paper.

The studied models include the possibility of the presence of an electrolyte between the conducting walls. It is generally believed that the long-ranged Casimir force between the fluctuating walls is screened by this electrolyte. Such an intuitively expected behaviour was supported longtime ago by an approximate Poisson-Boltzmann analysis of an electrolyte between two dielectric slabs [9]. A reasonable, but not rigorously justified, assumption was made: the electrostatic-field fluctuations in the walls, responsible for the long-ranged attractive Casimir force, can be treated separately from the pure image effects of the "inert" walls on the charged constituents of the electrolyte. Hereinafter, we refer to this assumption as the "separation hypothesis". Considering then the pure effect of images on the electrolyte particles, a repulsive long-ranged force of the same amplitude as the Casimir one, but in the opposite direction, occurs in the electrolyte. Following the basic separation hypothesis, the two long-ranged forces cancel exactly

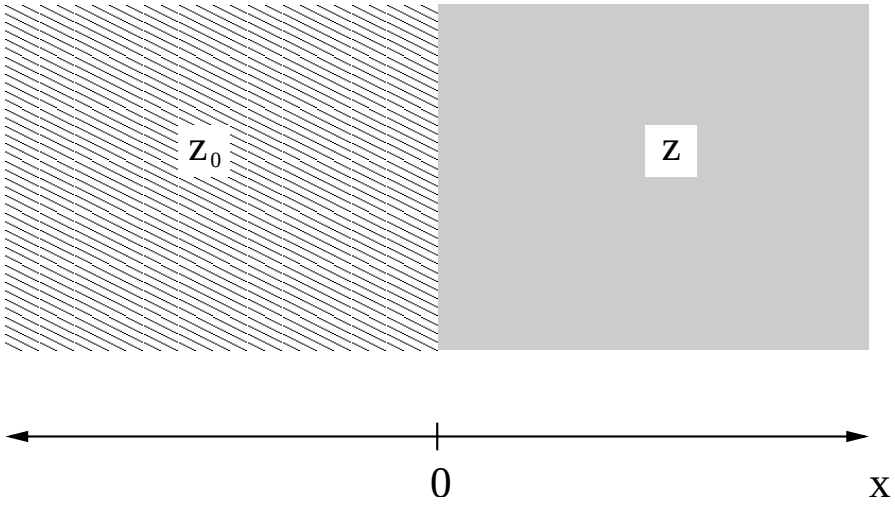

Figure 1. Polarizable interface.

with one another; we shall refer to this cancellation phenomenon as the screening effect. By the use of the separation hypothesis, this screening effect was also observed for an electrolyte between two conducting walls [10]. The presence of the repulsive long-ranged force in the electrolyte (modelled by the Coulomb gas) has been proven at arbitrary temperature, by using perfect-screening sum rules, for ideal-conductor [11] and ideal-dielectric [12] inert slab walls. Interestingly, in the special case when $\epsilon = 1$ (plain hard walls separating the electrolyte from vacuum), there is neither an attractive Casimir force between the slabs nor a repulsive force in the electrolyte induced by the particle images in the inert walls (in fact, there are no images). The corresponding field theory was developed in a series of works by Dean and Horgan [13].

In references [14, 15], and in a recent work [16] about the microscopic origin of universality in Casimir forces, the conducting walls in empty space are modelled by

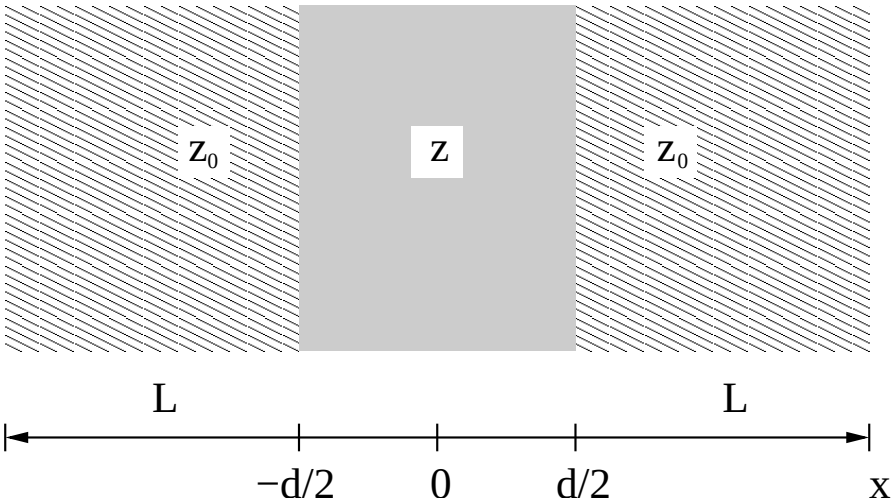

Figure 2. Two-slab geometry.

two slabs filled with a classical plasma of charged particles in thermal equilibrium. At large distances between the two slabs, the Casimir force (in the electrostatic regime) is retrieved as a result of perfect-screening sum rules. A natural continuation of the strategy is to replace the ideal conductor walls by a microscopic plasma system in more general physical situations.

The aim of the present paper is to study Casimir and related effects in model systems with geometries presented in figures 1 and 2, in which the confining walls are made of a symmetric two-component plasma (Coulomb gas) of point-like particles with $+/-$ unit charges in thermal equilibrium. The Coulomb gas is chosen for the sake of its simplicity; most of the obtained results can be easily generalized to multi-component plasmas. In the presence of an electrolyte (which is simply another Coulomb gas with a different particle fugacity) between the walls, the microscopic description of the walls enables us to mimic coherently the effect of electrostatic fluctuations inside the walls and the image forces acting on the electrolyte particles, without any ad-hoc separation ansatz. The wall-plasma is not required to be ideal, there might be a finite nonzero correlation length which describes the correlation effects among the charged particles.

If there is no electrolyte in the region between the two slabs (figure 2), the Casimir force is obtained in the limit of a large wall separation, together with a leading correction term due to the non-ideality of the conductor wall. If there is an electrolyte between the two slabs, the Casimir force is shown to be screened by this electrolyte, which confirms the validity of the separation (fluctuations-images) hypothesis. Interestingly, the residual short-ranged force between the slabs is always attractive. As a by-product of the treatment, we consider also the ideal-conductor regime of the walls when the correlation length of the charged particles forming the walls goes to zero. The surface tension of the electrolyte turns out to be independent of the electrostatic field fluctuations in the ideal-conductor walls. The analogous independence of the density profile and particle correlation functions was previously noted [17, 18].

The spatial dimension of the studied models will be $\nu = 2, 3$. In dimension ν, the Coulomb potential v at a spatial position $\mathbf{r}$, induced by a unit charge at the origin $\mathbf{0}$, is the solution of the Poisson equation

$$\Delta v(\mathbf{r}) = -s_\nu \delta(\mathbf{r}), \tag{1.1}$$

where $s_\nu = 2\pi^{\nu/2}/\Gamma(\nu/2)$ is the surface area of the ν-dimensional unit sphere. Explicitly,

$$v(\mathbf{r}) = \begin{cases} -\ln(r/a) & \text{if } \nu = 2, \\ r^{2-\nu}/(\nu-2) & \text{otherwise.} \end{cases} \tag{1.2}$$

Here, $r = |\mathbf{r}|$ and a is a free length scale. The definition (1.1) of the Coulomb potential implies in the Fourier space the characteristic small-k behaviour $\hat{v}(\mathbf{k}) \propto 1/k^2$ in any dimension. This maintains many generic properties (like screening [19]) of "real" 3D Coulomb systems. The interaction energy of charged particles $\{i, q_i = \pm 1\}$, immersed in a homogeneous medium of dielectric constant = 1, is $\sum_{i<j} q_i q_j v(|\mathbf{r}_i - \mathbf{r}_j|)$.

The models are treated in the grand canonical ensemble characterized by the inverse temperature β and by the couple of equivalent (there is no external electrostatic

potential) particle fugacities $z_+(\mathbf{r}) = z_-(\mathbf{r}) = z(\mathbf{r})$. The whole domain Λ on which the system is defined can be separated into disjunct subdomains, $\Lambda = \cup_\alpha \Lambda^{(\alpha)}$. Within the grand canonical formalism, each subdomain is characterized by a constant fugacity, $z_q(\mathbf{r}) = z^{(\alpha)}$ for $\mathbf{r} \in \Lambda^{(\alpha)}$, which may vary from one region to the other. The choice $z^{(\alpha)} = 0$ corresponds to a vacuum subdomain with no particles allowed to occupy the space. The grand partition function is defined by

$$\Xi = \sum_{N_+,N_-=0}^{\infty} \frac{1}{N_+!N_-!} \int \prod_{i=1}^{N} [\mathrm{d}^\nu r_i \, z_{q_i}(\mathbf{r}_i)] \exp\left[-\beta \sum_{i<j} q_i q_j v(|\mathbf{r}_i - \mathbf{r}_j|)\right], \tag{1.3}$$

where N_+ (N_-) is the number of positively (negatively) charged particles and $N = N_+ + N_-$. The averaged particle densities are generated from Ξ in a standard way as functional derivatives with respect to the fugacity field. At the one-particle level, one introduces the number density of particles of one sign,

$$n_q(\mathbf{r}) = \left\langle \sum_i \delta_{q,q_i} \delta(\mathbf{r} - \mathbf{r}_i) \right\rangle = \frac{1}{\Xi} \frac{\delta \Xi}{\delta z_q(\mathbf{r})}. \tag{1.4}$$

Due to the charge symmetry, $n_+(\mathbf{r}) = n_-(\mathbf{r}) = n(\mathbf{r})/2$ where n is the total density of particles. At the two-particle level, one introduces the two-body densities

$$\begin{aligned} n_{qq'}(\mathbf{r}, \mathbf{r}') &= \left\langle \sum_{i \neq j} \delta_{q,q_i} \delta(\mathbf{r} - \mathbf{r}_i) \delta_{q',q_j} \delta(\mathbf{r}' - \mathbf{r}_j) \right\rangle \\ &= \frac{1}{\Xi} \frac{\delta^2 \Xi}{\delta z_q(\mathbf{r}) \delta z_{q'}(\mathbf{r}')}. \end{aligned} \tag{1.5}$$

It is useful to consider also the (truncated) pair correlation functions

$$h_{qq'}(\mathbf{r}, \mathbf{r}') = \frac{n_{qq'}(\mathbf{r}, \mathbf{r}')}{n_q(\mathbf{r}) n_{q'}(\mathbf{r}')} - 1. \tag{1.6}$$

For the case of point-like particles, the singularity of the Coulomb potential (1.2) at the origin often prevents the thermodynamic stability against the collapse of positive-negative pairs of charges: in 2D for small enough temperatures, in 3D for any temperature. In particular, in 2D, the Boltzmann factor of a pair of $+/-$ unit charges, $r^{-\beta}$, is integrable at short distances provided that $\beta < 2$. To cross the collapse point $\beta = 2$, the pure Coulomb potential has to be regularized by a short-distance repulsion, e.g., a hard-core potential. In 3D, the short-distance regularization is needed at any temperature (except in the high-temperature limit described by the Debye-Hückel approximation which gives a thermodynamically stable description for point-like charges).

Two methods are applied. We first use the Debye-Hückel method of the Coulomb-bond chain resummation within the density Mayer expansion, valid in the high-temperature limit and applicable to both 2D and 3D systems. The standard approach dealing with inhomogeneous density profiles [20, 21] has to be supplemented by the first equation of the BGY hierarchy. We rather use the version developed in [22, 23] which does not require some additional information; we also introduce some technicalities which substantially simplify the calculation of the Casimir forces. We also use the

Debye-Hückel method in the case of dielectric walls, using the separation hypothesis which does not require any microscopic model for these walls. The second method applies exclusively to the 2D Coulomb gas whose exact solution (Ursell functions) can be obtained just at the collapse temperature $\beta = 2$ by a mapping onto the Thirring model at the free-fermion point [17, 24]. The free-fermion model is solvable also in many inhomogeneous situations and the corresponding method can be adapted to the present problems. The fact that, in 2D, one can verify whether some features of the mean-field behaviour predicted by the Debye-Hückel analysis persist also at a specific finite temperature is of importance. We add that, based on a recent progress in the integrable $1+1$ dimensional Quantum Field Theory [25, 26], the thermodynamics of the 2D Coulomb gas was solved exactly in the whole stability region $\beta < 2$, in the bulk [27] as well as for interface geometries with an ideal-conductor [28] and an ideal-dielectric [29] walls; however, for $\beta < 2$, the exact n-body densities are not known, and we shall not consider the case $\beta < 2$ in the present paper.

The paper is organized as follows. In section 2, for the two-slab geometry (figure 2) with general dielectric walls, by using a phenomenological approach, it is shown, under certain conditions, that the electric field fluctuations can be decoupled from the image-particle forces. The separation hypothesis is then tested on the microscopic models, first in the Debye-Hückel limit (section 3) and then at the free-fermion point of the Thirring representation of the 2D Coulomb gas (section 4). A brief recapitulation and concluding remarks are given in section 5.

2. Phenomenology

2.1. The separation hypothesis

A general argument in favour of the separation hypothesis has been given in the case of conducting walls [15]. After a minor modification, the same argument can be used for dielectric walls of arbitrary dielectric constant ϵ. For the sake of completeness, we repeat the argument.

We consider, in ν dimensions, a Coulomb gas partially or totally bounded by walls W made of a dielectric with a dielectric constant ϵ. We want to take into account the thermal fluctuations of the walls. It happens that a detailed knowledge of the internal structure of the walls is not necessary; we only assume that this internal structure is described by a set of coordinates $\{\mathbf{R}\}$. Classical (non-quantum) statistical mechanics is supposed to be applicable.

We shall need a correlation function defined for the wall system supposed to be alone in space. Let $\Phi_W(\mathbf{r})$ be the electric potential created by the walls at some point $\mathbf{r}$ and let $\langle \Phi_W(\mathbf{r})\Phi_W(\mathbf{r}')\rangle_0^{\mathrm{T}}$ be a truncated statistical average computed with the Boltzmann weight of the walls alone. This correlation function, when both $\mathbf{r}$ and $\mathbf{r}'$ are outside the walls, can be computed by linear response theory, by a simple adaptation of reference [30]. Let us put a point charge q at $\mathbf{r}'$. Its interaction with the walls results into the

addition to the Hamiltonian of a term $\delta H = q\Phi_W(\mathbf{r}')$. The average electric potential at $\mathbf{r}$ is changed by $qG(\mathbf{r},\mathbf{r}')$ with G determined by macroscopic electrostatics. For instance, in the case of one plane wall, $G(\mathbf{r},\mathbf{r}') = v(\mathbf{r}-\mathbf{r}') + [(1-\epsilon)/(1+\epsilon)]v(\mathbf{r}-\mathbf{r}'^*)$ where v is the Coulomb interaction (1.2) and $\mathbf{r}'^*$ is the image of $\mathbf{r}'$.

Let $-G^*$ be that part of G due to the walls (not to q itself):

$$-G^*(\mathbf{r},\mathbf{r}') = G(\mathbf{r},\mathbf{r}') - v(\mathbf{r}-\mathbf{r}'). \tag{2.1}$$

If q is infinitesimal, linear response theory states that $-qG^* = -\beta\langle\Phi_W(\mathbf{r})\delta H\rangle_0^{\mathrm{T}}$, therefore

$$\beta\langle\Phi_W(\mathbf{r})\Phi_W(\mathbf{r}')\rangle_0^{\mathrm{T}} = G^*(\mathbf{r},\mathbf{r}'). \tag{2.2}$$

Furthermore, we can assume that the fluctuations of $\Phi_W(\mathbf{r})$ are Gaussian, because, in a macroscopic description with a constant ϵ, the response of the walls to the external charge q is linear even for a non-infinitesimal charge (if the response of a spring to an applied force is linear, it means that the spring is harmonic, and its spontaneous thermal fluctuations will be Gaussian).

We now come back to the full system Coulomb gas plus walls, the partition function of which will be considered. Let $H_0(\{\mathbf{R}\})$ be the potential energy of the walls, $\{\mathbf{r}\}$ the set of the particle coordinates of of the Coulomb gas. The total potential energy of the system (Coulomb gas plus W) is

$$H(\{\mathbf{r}\},\{\mathbf{R}\}) = \sum_i q_i\Phi_W(\mathbf{r}_i,\{\mathbf{R}\}) + \sum_{i<j} q_iq_jv(\mathbf{r}_i-\mathbf{r}_j) + H_0(\{\mathbf{R}\}), \tag{2.3}$$

where q_i and $\mathbf{r}_i$ are the charge and coordinates of the ith particle of the Coulomb gas. Let $\mathrm{d}\Gamma$ the phase space element (after integration on the momenta) of the Coulomb gas. The partition function Z of the total system can be written as

$$Z = Z_0\int \mathrm{d}\Gamma \left\langle \exp\left[-\beta\sum_i q_i\Phi_W(\mathbf{r}_i,\{\mathbf{R}\})\right]\right\rangle_0 \exp\left[-\beta\sum_{i<j} q_iq_jv(\mathbf{r}_i-\mathbf{r}_j)\right], \tag{2.4}$$

where $\langle\cdots\rangle_0$ means the average over $\{\mathbf{R}\}$ with the weight $\exp[-\beta H_0]$, and Z_0 is the partition function of the walls alone. Since the fluctuations of Φ_W are Gaussian and $\langle\Phi_W(\mathbf{r})\rangle_0 = 0$,

$$\begin{aligned}\left\langle \exp\left[-\beta\sum_i q_i\Phi_W(\mathbf{r}_i,\{\mathbf{R}\})\right]\right\rangle_0 &= \exp\left[\tfrac{1}{2}\beta^2\sum_{i,j} q_iq_j\langle\Phi_W(\mathbf{r}_i)\Phi_W(\mathbf{r}_j)\rangle_0^{\mathrm{T}}\right]\\ &= \exp\left[\tfrac{1}{2}\beta\sum_{i,j} q_iq_jG^*(\mathbf{r}_i,\mathbf{r}_j)\right].\end{aligned} \tag{2.5}$$

Thus, the partition function can be factorized (separated) as

$$Z = Z_{\mathrm{eff}}Z_0, \tag{2.6}$$

where Z_{eff} is the partition function of the Coulomb gas computed with the effective Hamiltonian

$$H_{\mathrm{eff}} = -\frac{1}{2}\sum_i q_i^2G^*(\mathbf{r}_i,\mathbf{r}_i) + \sum_{i<j} q_iq_jG(\mathbf{r}_i,\mathbf{r}_j). \tag{2.7}$$

$H_{\rm eff}$ is the standard Hamiltonian of a Coulomb gas in presence of inert dielectric walls. For instance, in the case of one plane dielectric wall, the first term of $H_{\rm eff}$ is the interaction of each particle with its own image, while the second term is the interaction of each particle with the other ones and the images of the other ones.

Let $A(\{\mathbf{r}\})$ be any microscopic quantity which does not depend on $\{\mathbf{R}\}$. Using the same kind of steps as for the calculation of the partition function Z, one can show that this average can be calculated with $H_{\rm eff}$ only:

$$\langle A\rangle = \frac{1}{Z_{\rm eff}}\int {\rm d}\Gamma \exp(-\beta H_{\rm eff})A. \tag{2.8}$$

In particular, the densities and many-body correlations in the Coulomb gas can be calculated with $H_{\rm eff}$ and therefore are unaffected by the fluctuations in the walls.

On the contrary, the total partition function (2.6) does involve Z_0, and therefore the fluctuations in the walls enter the total free energy; if a wall is displaced, the variation of the free energy, and therefore the force acting on this wall, will be affected by the fluctuations in the walls.

In the above, simple manipulations allow to replace the partition function $Z_{\rm eff}$ of the Coulomb gas by the corresponding grand partition function $\Xi_{\rm eff}$ also computed with the Hamiltonian $H_{\rm eff}$. Therefore, the grand potential of the total system is

$$\Omega = \Omega_{\rm eff} + F_0, \tag{2.9}$$

where $\Omega_{\rm eff}$ is the grand potential of the Coulomb gas computed with the Hamiltonian $H_{\rm eff}$ and F_0 is the free energy of the wall system alone in space.

Furthermore, we have considered the case when the Coulomb gas is made of charged particles in vacuum. A more realistic model for an electrolyte takes into account the solvent by picturing it as a continuous dielectric medium with a dielectric constant ϵ_S. Then, in the above, ϵ means the ratio ϵ_W/ϵ_S where now ϵ_W is the dielectric constant of the walls.

In the limit $\epsilon \to \infty$, the results about conducting walls [15] are retrieved.

2.2. Casimir force between two dielectric walls

In the present subsection, we give a simple argument for computing the Casimir force between two parallel dielectric walls separated by vacuum. We work in ν dimensions. The walls, perpendicular to the x axis, modelled as media with a dielectric constant ϵ, occupy the regions $x > d/2$ and $x < -d/2$. The slab $-d/2 < x < d/2$ is empty. Each point $\mathbf{r}$ is defined by its Cartesian coordinates $(x, \mathbf{r}^\perp)$ where $\mathbf{r}^\perp$ is the $(\nu-1)$ dimensional vector perpendicular to the x axis. We shall compute the average xx component of the Maxwell stress tensor [31] in the empty region.

Let $G(\mathbf{r}, \mathbf{r}')$ be the electric potential at $\mathbf{r}$ when a unit charge is placed at the source point $\mathbf{r}'$ in the empty region. Macroscopic electrostatics gives for G the equations

$$\Delta G(\mathbf{r}, \mathbf{r}') = \begin{cases} -s_\nu \delta(\mathbf{r}-\mathbf{r}') & \text{if } -d/2 < x < d/2\ , \\ 0 & \text{if } x < -d/2 \text{ or } x > d/2\ , \end{cases} \tag{2.10}$$

with the conditions that G and $\epsilon(\partial G/\partial x)$ [with $\epsilon = 1$ if $-d/2 < x < d/2$] be continuous at $x = -d/2$ and $x = d/2$, and that $G \to 0$ when $x \to \pm\infty$. The standard technique is to use the Fourier transform $\hat{G}$ in the $\mathbf{r}^\perp$ space, defined as in (3.15). A derivation similar to the ones in section 3 gives for G^*, defined by (2.1), the Fourier transform $\hat{G}^*$

$$\hat{G}^* = -\frac{s_\nu}{l}\left\{\cosh[l(x-x')]\left[\left(\frac{1+\epsilon}{1-\epsilon}\right)^2 \mathrm{e}^{2ld} - 1\right]^{-1} + \cosh[l(x+x')]\left[\left(\frac{1+\epsilon}{1-\epsilon}\right)\mathrm{e}^{ld} - \left(\frac{1-\epsilon}{1+\epsilon}\right)\mathrm{e}^{-ld}\right]^{-1}\right\}. \tag{2.11}$$

The xx component T_{xx} of the average Maxwell stress tensor at $\mathbf{r}$ is, from (2.2) with $\langle\Phi_W(\mathbf{r})\rangle = 0$,

$$T_{xx}(\mathbf{r}) = \frac{\beta^{-1}}{2s_\nu}\left[\frac{\partial^2}{\partial x \partial x'} - \nabla_{\mathbf{r}^\perp}\cdot\nabla_{\mathbf{r}'^\perp}\right] G^*(\mathbf{r},\mathbf{r}')\Big|_{\mathbf{r}'=\mathbf{r}}. \tag{2.12}$$

When G^* is expressed in terms of its Fourier transform (2.11), (2.12) becomes

$$\begin{aligned}\beta T_{xx} &= \frac{s_{\nu-1}}{(2\pi)^{\nu-1}}\int_0^\infty \mathrm{d}l\, l^{\nu-1}\left[\left(\frac{1+\epsilon}{1-\epsilon}\right)^2 \mathrm{e}^{2ld} - 1\right]^{-1} \\ &= \frac{s_{\nu-1}}{(2\pi)^{\nu-1}(2d)^\nu}\left(\frac{1-\epsilon}{1+\epsilon}\right)^2 \Gamma(\nu)\Phi\left(\left(\frac{1-\epsilon}{1+\epsilon}\right)^2, \nu, 1\right),\end{aligned} \tag{2.13}$$

where Φ is the Lerch function [32]

$$\Phi(z,\nu,1) = \sum_{n=1}^\infty \frac{z^{n-1}}{n^\nu}. \tag{2.14}$$

$-T_{xx}$ is independent of $\mathbf{r}$. It is the force per unit area, measured along the x-axis, which acts on the right wall. This force is attractive. It is related to the free energy of the wall system F_0 introduced in section 2.1 by

$$-T_{xx} = -\frac{1}{\mathcal{A}}\frac{\partial F_0}{\partial d}, \tag{2.15}$$

where $\mathcal{A}$ is the area of each wall.

If $\nu = 3$, (2.13) is in agreement with Lifshitz [3]. In the limit of conducting walls $\epsilon \to \infty$, it reduces to $\beta T_{xx} = \zeta(3)/(8\pi d^3)$, where ζ is the Riemann zeta function. This is indeed the correct electrostatic part of the Casimir force between conducting walls in the classical limit [4, 14].

If $\nu = 2$, in the limit of conducting walls, $\beta T_{xx} = \pi/(24d^2)$, in agreement with a previous result [14].

3. Debye-Hückel theory

The weak-coupling (high-temperature) limit of a Coulomb system is described by the Debye-Hückel theory.

3.1. General formalism

We first consider the bulk regime when the Coulomb system is defined in the whole space, $\Lambda = R^\nu$, and the fugacities $\{z_q\}$ of particles with charges $q \in Q$ as well as the corresponding particle densities $\{n_q\}$ are constant in space. A consistent way of deriving the Debye-Hückel theory is to start with the diagrammatic Mayer expansion in density. Summing up the chain diagrams leads to the renormalized bonds, and the cluster integrals converge in the renormalized format (see, for instance, [23, 27]). This is equivalent to writing the Ornstein-Zernicke (OZ) equations for the pair correlation function (1.6) with the direct correlation function replaced by $-\beta$ times the corresponding interaction potential:

$$h_{q_1q_2}(\mathbf{r}_1,\mathbf{r}_2) = -\beta q_1 q_2 v(|\mathbf{r}_1-\mathbf{r}_2|) + \sum_{q_3}\int_\Lambda \mathrm{d}^\nu r_3 \left[-\beta q_1 q_3 v(|\mathbf{r}_1-\mathbf{r}_3|)\right] n_{q_3}(\mathbf{r}_3) h_{q_3q_2}(\mathbf{r}_3,\mathbf{r}_2) \tag{3.1}$$

The solution is of the form

$$h_{q_1q_2}(\mathbf{r}_1,\mathbf{r}_2) = -\beta q_1 q_2 G(\mathbf{r}_1,\mathbf{r}_2), \tag{3.2}$$

where G obeys the integral equation

$$G(\mathbf{r}_1,\mathbf{r}_2) = v(|\mathbf{r}_1-\mathbf{r}_2|) - \frac{\kappa^2}{s_\nu}\int_\Lambda \mathrm{d}^\nu r_3 v(|\mathbf{r}_1-\mathbf{r}_3|) G(\mathbf{r}_3,\mathbf{r}_2). \tag{3.3}$$

Here, κ is the inverse Debye length defined by $\kappa^2 = s_\nu \beta \sum_q n_q q^2$. The integral equation (3.3) can be transformed into a differential equation by taking the Laplacian with respect to $\mathbf{r}_1$. In this way one arrives at the usual Debye-Hückel equation

$$\left[\Delta_1 - \kappa^2\right] G(\mathbf{r}_1,\mathbf{r}_2) = -s_\nu \delta(\mathbf{r}_1-\mathbf{r}_2) \tag{3.4}$$

which has to be supplemented by the vanishing boundary conditions for the screened Coulomb potential G when $|\mathbf{r}_1-\mathbf{r}_2| \to \infty$. The bulk density-fugacity relationship can be obtained by using the formula

$$n_q = z_q \exp\left\{\frac{\beta q^2}{2}\lim_{r\to 0}\left[-G(r)+v(r)\right]\right\}. \tag{3.5}$$

The specific grand partition function can be calculated from the standard relation

$$n_q = z_q \frac{\partial}{\partial z_q}\frac{\ln\Xi}{|\Lambda|} \tag{3.6}$$

with the condition $\ln\Xi = 0$ at $\{z_q = 0\}$. The bulk pressure p is given by $\beta p = \ln\Xi/|\Lambda|$.

In the 2D Coulomb gas, the screened Coulomb potential is found in the form

$$G(r) = K_0(\kappa r), \qquad \kappa = (2\pi\beta n)^{1/2} \qquad (\nu = 2), \tag{3.7}$$

where K_0 is a modified Bessel function. Using the small-x expansion of $K_0(x)$ [32]

$$K_0(x) = -\ln\left(\frac{x}{2}\right) - C + O(x^2 \ln x) \tag{3.8}$$

with C being the Euler's constant, the density-fugacity relationship (3.5) reads

$$\frac{n^{1-\beta/4}}{z a^{\beta/2}} = 2\left(\frac{\pi\beta}{2}\right)^{\beta/4}\exp\left(\frac{\beta C}{2}\right). \tag{3.9}$$

The bulk pressure is given by $\beta p = (1 - \beta/4)n$. This equation of state turns out to be valid for any $\beta \leq 2$.

In the 3D Coulomb gas, the screened Coulomb potential is found in the form

$$G(r) = \frac{\exp(-\kappa r)}{r}, \qquad \kappa = (4\pi\beta n)^{1/2} \qquad (\nu = 3) \tag{3.10}$$

The density-fugacity relationship then reads

$$n = 2\left[z + \sqrt{2\pi}(\beta z)^{3/2}\right]. \tag{3.11}$$

The bulk pressure is given by $\beta p = n - \kappa^3/(24\pi)$.

The above Debye-Hückel theory can be straightforwardly extended to inhomogeneous situations when the system domain Λ is separated into disjunct subdomains, $\Lambda = \cup_\alpha \Lambda^{(\alpha)}$. Each subdomain is characterized by constant fugacities, $z_q(\mathbf{r}) = z_q^{(\alpha)}$ for $\mathbf{r} \in \Lambda^{(\alpha)}$, and the corresponding bulk densities $n_q^{(\alpha)}$. At the lowest level, the densities in the OZ equations (3.1) are taken constant (equal to the bulk ones) within each of the subdomains, $n_q(\mathbf{r}) = n_q^{(\alpha)}$ for $\mathbf{r} \in \Lambda^{(\alpha)}$. The solution of the OZ equations is again of the form (3.2), where the screened Coulomb potential G obeys the integral equation

$$G(\mathbf{r}_1, \mathbf{r}_2) = v(|\mathbf{r}_1 - \mathbf{r}_2|) - \sum_\alpha \frac{\kappa_\alpha^2}{s_\nu} \int_{\Lambda^{(\alpha)}} \mathrm{d}^\nu r_3 v(|\mathbf{r}_1 - \mathbf{r}_3|) G(\mathbf{r}_3, \mathbf{r}_2). \tag{3.12}$$

Here, κ_α is the inverse Debye length for the subdomain $\Lambda^{(\alpha)}$ defined by $\kappa_\alpha^2 = s_\nu \beta \sum_q n_q^{(\alpha)} q^2$. Equivalently,

$$\left[\Delta_1 - \kappa_\alpha^2\right] G(\mathbf{r}_1, \mathbf{r}_2) = -s_\nu \delta(\mathbf{r}_1 - \mathbf{r}_2), \qquad \mathbf{r}_1 \in \Lambda^{(\alpha)}, \tag{3.13}$$

where the spatial position of the source point $\mathbf{r}_2$ is arbitrary. Since, according to (3.12), G is proportional to v, these equations must be supplemented by the usual electrostatic conditions at each subdomain boundary $\partial\Lambda^{(\alpha)}$: G and its normal derivative with respect to the boundary surface $\partial_\perp G$ are continuous at $\partial\Lambda^{(\alpha)}$. The leading β-correction to the particle densities in a given subdomain is determined by the inhomogeneous counterpart of equation (3.5),

$$n_q^{(\alpha)}(\mathbf{r}) = z_q^{(\alpha)} \exp\left\{\frac{\beta q^2}{2} \lim_{\mathbf{r}' \to \mathbf{r}} \left[-G(\mathbf{r}, \mathbf{r}') + v(\mathbf{r}, \mathbf{r}')\right]\right\} \tag{3.14}$$

where $\mathbf{r} \in \Lambda^{(\alpha)}$.

3.2. Polarizable interface

The model is an infinite Coulomb gas of point unit charges $q = \pm 1$, separated by an interface (perpendicular to the x axis and localized at $x = 0$) into two half spaces $x > 0$ and $x < 0$ (see figure 1). Each point $\mathbf{r} \in R^\nu$ is thus defined by Cartesian coordinates $\mathbf{r} = (x, \mathbf{r}^\perp)$, where $\mathbf{r}^\perp$ is the $(\nu - 1)$ dimensional vector component perpendicular to the x axis. The particle fugacities are, in general, different on each side of the interface, $z_q(\mathbf{r}) = z$ when $x > 0$ and $z_q(\mathbf{r}) = z_0$ when $x < 0$. The corresponding bulk (total number) densities and inverse Debye lengths will be denoted by (n, κ) and (n_0, κ_0). Since

the system is translationally invariant in the perpendicular $\mathbf{r}^{\perp}$-subspace, the standard technique is to use the Fourier transform

$$G(\mathbf{r}_1,\mathbf{r}_2)=\int\frac{\mathrm{d}^{\nu-1}l}{(2\pi)^{\nu-1}}\hat{G}(x_1,x_2;\mathbf{l})\exp\left\{\mathrm{i}\mathbf{l}\cdot(\mathbf{r}_1^{\perp}-\mathbf{r}_2^{\perp})\right\} \tag{3.15}$$

We want to solve equations (3.13) when, for instance, the source point $\mathbf{r}_2=(x_2,\mathbf{r}_2^{\perp})$ has the coordinate $x_2>0$. In terms of the Fourier component $\hat{G}$ one obtains ordinary differential equations in one variable:

$$\left(\frac{\partial^2}{\partial x_1^2}-\kappa^2-l^2\right)\hat{G}(x_1,x_2;\mathbf{l})=-s_\nu\delta(x_1-x_2),\qquad(x_1>0), \tag{3.16a}$$

$$\left(\frac{\partial^2}{\partial x_1^2}-\kappa_0^2-l^2\right)\hat{G}(x_1,x_2;\mathbf{l})=0,\qquad(x_1<0). \tag{3.16b}$$

We look for a solution, vanishing at $x_1\to\pm\infty$, of the form

$$\hat{G}=\frac{s_\nu}{2\sqrt{\kappa^2+l^2}}\exp\left(-\sqrt{\kappa^2+l^2}|x_1-x_2|\right)$$
$$+A_l\exp\left[-\sqrt{\kappa^2+l^2}(x_1+x_2)\right],\qquad(x_1>0), \tag{3.17a}$$

$$\hat{G}=B_l\exp\left(\sqrt{\kappa_0^2+l^2}x_1-\sqrt{\kappa^2+l^2}x_2\right),\qquad(x_1<0). \tag{3.17b}$$

The constants A_l and B_l are determined by the conditions that $\hat{G}$ and $\partial\hat{G}/\partial x_1$ are continuous at $x_1=0$. The result is

$$A_l=\frac{s_\nu}{2\sqrt{\kappa^2+l^2}}\frac{\sqrt{\kappa^2+l^2}-\sqrt{\kappa_0^2+l^2}}{\sqrt{\kappa^2+l^2}+\sqrt{\kappa_0^2+l^2}}, \tag{3.18a}$$

$$B_l=s_\nu\frac{1}{\sqrt{\kappa^2+l^2}+\sqrt{\kappa_0^2+l^2}}. \tag{3.18b}$$

The leading β-correction to the constant particle density can now be calculated for $x>0$ by using a linearization in (3.14). Considering $x_1,x_2>0$, the first term on the rhs of (3.17a) contributes to the bulk density-fugacity relationship, while the second term implies

$$n(x)=n\left[1-\frac{\beta}{2}\int\frac{\mathrm{d}^{\nu-1}l}{(2\pi)^{\nu-1}}A_l\exp\left(-2\sqrt{\kappa^2+l^2}x\right)\right]. \tag{3.19}$$

More explicitly, one has

$$n(x)-n=\frac{\kappa^2 s_{\nu-1}}{4(2\pi)^{\nu-1}}\int_0^\infty\frac{\mathrm{d}l\,l^{\nu-2}}{\sqrt{\kappa^2+l^2}}\frac{\sqrt{\kappa_0^2+l^2}-\sqrt{\kappa^2+l^2}}{\sqrt{\kappa_0^2+l^2}+\sqrt{\kappa^2+l^2}}\exp\left(-2\sqrt{\kappa^2+l^2}x\right) \tag{3.20}$$

for the density profile at $x>0$. The same method applies when the source point $\mathbf{r}_2=(x_2,\mathbf{r}_2^{\perp})$ has the component $x_2<0$, with the final result

$$n_0(x)-n_0=\frac{\kappa_0^2 s_{\nu-1}}{4(2\pi)^{\nu-1}}\int_0^\infty\frac{\mathrm{d}l\,l^{\nu-2}}{\sqrt{\kappa_0^2+l^2}}\frac{\sqrt{\kappa^2+l^2}-\sqrt{\kappa_0^2+l^2}}{\sqrt{\kappa^2+l^2}+\sqrt{\kappa_0^2+l^2}}\exp\left(2\sqrt{\kappa_0^2+l^2}x\right) \tag{3.21}$$

for the density profile at $x<0$.

For the present geometry, the grand potential $\Omega = -\beta^{-1} \ln \Xi$ is the sum of a volume part and a surface part,

$$\Omega = -\frac{|\Lambda|}{2} \left[p(z) + p(z_0) \right] + |\partial\Lambda| \gamma(z, z_0), \tag{3.22}$$

where $|\partial\Lambda|$ stands for the interface area and γ for the surface tension. The total number of particles is given by

$$N = z \frac{\partial(-\beta\Omega)}{\partial z} + z_0 \frac{\partial(-\beta\Omega)}{\partial z_0}. \tag{3.23}$$

The surface parts of this relation read [17]

$$z \frac{\partial(-\beta\gamma)}{\partial z} = \int_0^\infty \mathrm{d}x \left[n(x) - n \right], \tag{3.24a}$$

$$z_0 \frac{\partial(-\beta\gamma)}{\partial z_0} = \int_{-\infty}^0 \mathrm{d}x \left[n_0(x) - n_0 \right]. \tag{3.24b}$$

The surface tension is zero in the homogeneous bulk regime,

$$\beta\gamma(z, z_0) = 0 \quad \text{when } z = z_0. \tag{3.25}$$

At the lowest order in β, $z\partial_z$ and $z_0\partial_{z_0}$ can be replaced respectively by $n\partial_n$ and $n_0\partial_{n_0}$. Having at one's disposal the density profiles, equations (3.20) and (3.21), after some algebra one finally arrives at

$$\beta\gamma = \frac{s_{\nu-1}}{4(2\pi)^{\nu-1}} \int_0^\infty \mathrm{d}l \, l^{\nu-2} \ln \left[\frac{\left(\sqrt{\kappa_0^2 + l^2} + \sqrt{\kappa^2 + l^2} \right)^2}{4\sqrt{\kappa_0^2 + l^2}\sqrt{\kappa^2 + l^2}} \right]. \tag{3.26}$$

Note that the argument of the logarithm behaves like $1 + O(1/l^4)$ for large l, so the integral is finite in both $\nu = 2$ and 3 dimensions of interest. When there are no particles at the half-space $x < 0$, i.e. $\kappa_0 = 0$, the relations

$$\beta\gamma^{(\mathrm{vac})}(\kappa) = \begin{cases} \dfrac{\kappa}{8\pi}(4 - \pi), & \nu = 2 \\ \dfrac{\kappa^2}{32\pi}(2\ln 2 - 1), & \nu = 3 \end{cases} \tag{3.27}$$

define the surface tension of the plasma in contact with a vacuum (plain hard wall with $\epsilon = 1$) [33].

We now aim at studying the formula (3.26) in the ideal-conductor limit when the correlation length of the charged particles, say in the half-space $x < 0$, goes to zero, i.e. $\kappa_0 \to \infty$. The analysis depends on the spatial dimension.

- In 2D, the large-κ_0 expansion of (3.26) results in a decomposition

$$\beta\gamma = \frac{\kappa_0}{8\pi}(4 - \pi) - \frac{\kappa}{8} + \beta\gamma_{\mathrm{mix}} \tag{3.28}$$

where

$$\beta\gamma_{\mathrm{mix}} = \frac{\kappa_0}{2\pi} \int_0^\infty \mathrm{d}k \ln \left[\frac{\sqrt{1 + k^2} + \sqrt{(\kappa/\kappa_0)^2 + k^2}}{\sqrt{1 + k^2} + k} \right]. \tag{3.29}$$

On the rhs of (3.28), the first term corresponds to the vacuum surface tension of the Coulomb gas in the half-space $x < 0$ (owing to $\kappa_0 >> \kappa$, the relatively sparse Coulomb gas localized at $x > 0$ is in fact seen as vacuum) and the second term corresponds to the surface tension of the Coulomb gas in the half-space $x > 0$ in the presence of an inert ideal-conductor wall [28]. The last term, defined by (3.29), represents the "mixing" of the two surface tensions. It can be further simplified, via successive integrations by parts, to the form

$$\beta\gamma_{\rm mix} = \frac{\kappa_0}{2\pi}\left\{\frac{\kappa}{\kappa_0}\mathbf{E}\left[1-\left(\frac{\kappa_0}{\kappa}\right)^2\right]-1\right\}, \tag{3.30}$$

where $\mathbf{E}$ is a complete elliptic integral. In the limit $\kappa/\kappa_0 \to 0$, one has

$$\frac{\beta\gamma_{\rm mix}}{\kappa} = -\frac{1}{4\pi}\frac{\kappa}{\kappa_0}\ln\left(\frac{\kappa}{\kappa_0}\right) + O\left(\frac{\kappa}{\kappa_0}\right), \tag{3.31}$$

so that the mixing surface tension vanishes in the ideal-conductor limit. This means that the electrostatic field fluctuations in the wall do not modify the surface tension $-\kappa/8$ calculated with an inert ideal-conductor wall.

- In 3D, the integral in equation (3.26) can be evaluated explicitly,

$$\beta\gamma = \frac{1}{16\pi}\left[-\frac{1}{2}(\kappa_0-\kappa)^2 + \kappa_0^2\ln\left(\frac{2\kappa_0}{\kappa_0+\kappa}\right) + \kappa^2\ln\left(\frac{2\kappa}{\kappa_0+\kappa}\right)\right]. \tag{3.32}$$

In the limit $\kappa/\kappa_0 \to 0$,

$$\beta\gamma = \frac{\kappa_0^2}{32\pi}(2\ln 2 - 1) + \frac{\kappa^2}{16\pi}\ln\left(\frac{2\kappa}{\kappa_0}\right) + \beta\gamma_{\rm mix}, \tag{3.33}$$

where the mixing surface tension is given by the expansion formula

$$\frac{\beta\gamma_{\rm mix}}{\kappa^2} = -\frac{1}{12\pi}\left(\frac{\kappa}{\kappa_0}\right) + O\left[\left(\frac{\kappa}{\kappa_0}\right)^2\right]. \tag{3.34}$$

Like in 2D, the first term on the rhs of (3.33) is the vacuum surface tension of the Coulomb gas in the half-space $x < 0$. The second term, the surface tension of the Coulomb gas in the half-space $x > 0$ due to the conductor wall, diverges in the ideal-conductor limit. On the other hand, the mixing surface tension vanishes in the ideal-conductor limit.

3.3. Two-slab geometry

The model consists of two slabs (see figure 2) modelled by Coulomb gases with the same bulk characteristics (n_0, κ_0). The slabs have thickness L and are separated by a distance d:

$$\Lambda_- = \left\{\mathbf{r} = (x, \mathbf{r}^\perp) | x \in X_- = \langle -d/2 - L, -d/2\rangle, \mathbf{r}^\perp \in R^{\nu-1}\right\},$$
$$\Lambda_+ = \left\{\mathbf{r} = (x, \mathbf{r}^\perp) | x \in X_+ = \langle d/2, d/2 + L\rangle, \mathbf{r}^\perp \in R^{\nu-1}\right\}.$$

There is an electrolyte, modelled simply by another Coulomb gas with different bulk characteristics (n, κ), in the region $(X_0 = \langle -d/2, d/2\rangle) \times R^{\nu-1}$ between the slabs; the choice $n = \kappa = 0$ corresponds to vacuum between the slabs. The remaining external

space to the slabs is supposed to be vacuum. The thickness L of the slabs is large enough to screen the boundary effects at $x = \pm d/2$, so that the opposite boundaries have the density characteristics identical to those close to a plain hard wall.

Let the source point $\mathbf{r}_2 = (x_2, \mathbf{r}_2^{\perp})$ have the coordinate $x_2 \in X_+$. In terms of the Fourier component $\hat{G}$, equations (3.13) take the form

$$\left(\frac{\partial^2}{\partial x_1^2} - \kappa_0^2 - l^2\right)\hat{G}(x_1, x_2; \mathbf{l}) = -s_\nu \delta(x_1 - x_2), \qquad (x_1 \in X_+), \qquad (3.35a)$$

$$\left(\frac{\partial^2}{\partial x_1^2} - \kappa^2 - l^2\right)\hat{G}(x_1, x_2; \mathbf{l}) = 0, \qquad (x_1 \in X_0), \qquad (3.35b)$$

$$\left(\frac{\partial^2}{\partial x_1^2} - \kappa_0^2 - l^2\right)\hat{G}(x_1, x_2; \mathbf{l}) = 0, \qquad (x_1 \in X_-). \qquad (3.35c)$$

In the limit $L \to \infty$, we look for a solution, vanishing at $x_1 \to \pm\infty$, of the form

$$\hat{G} = \frac{s_\nu}{2\sqrt{\kappa_0^2 + l^2}} \exp\left(-\sqrt{\kappa_0^2 + l^2}|x_1 - x_2|\right) + A_l \exp\left[-\sqrt{\kappa_0^2 + l^2}(x_1 + x_2)\right], \qquad (x_1 \in X_+), \qquad (3.36a)$$

$$\hat{G} = \exp\left(-\sqrt{\kappa_0^2 + l^2}x_2\right)\left[B_l \exp\left(\sqrt{\kappa^2 + l^2}x_1\right) + C_l \exp\left(-\sqrt{\kappa^2 + l^2}x_1\right)\right], \qquad (x_1 \in X_0), \qquad (3.36b)$$

$$\hat{G} = D_l \exp\left[\sqrt{\kappa_0^2 + l^2}(x_1 - x_2)\right], \qquad (x_1 \in X_-). \qquad (3.36c)$$

The constants A_l, B_l, C_l and D_l are determined by the conditions that $\hat{G}$ and $\partial\hat{G}/\partial x_1$ are continuous at $x_1 = \pm d/2$. Introducing the auxiliary function

$$W(l) = \left[(\kappa_0^2 + l^2) + (\kappa^2 + l^2)\right]\sinh\left(\sqrt{\kappa^2 + l^2}d\right) + 2\sqrt{\kappa_0^2 + l^2}\sqrt{\kappa^2 + l^2}\cosh\left(\sqrt{\kappa^2 + l^2}d\right), \qquad (3.37)$$

one finds

$$A_l = \frac{s_\nu}{2W(l)}\frac{\kappa_0^2 - \kappa^2}{\sqrt{\kappa_0^2 + l^2}}\exp\left(\sqrt{\kappa_0^2 + l^2}d\right)\sinh\left(\sqrt{\kappa^2 + l^2}d\right), \qquad (3.38a)$$

$$B_l = \frac{s_\nu}{2W(l)}\left(\sqrt{\kappa_0^2 + l^2} + \sqrt{\kappa^2 + l^2}\right)\exp\left[\left(\sqrt{\kappa_0^2 + l^2} + \sqrt{\kappa^2 + l^2}\right)\frac{d}{2}\right], \qquad (3.38b)$$

$$C_l = -\frac{s_\nu}{2W(l)}\left(\sqrt{\kappa_0^2 + l^2} - \sqrt{\kappa^2 + l^2}\right)\exp\left[\left(\sqrt{\kappa_0^2 + l^2} - \sqrt{\kappa^2 + l^2}\right)\frac{d}{2}\right]. \qquad (3.38c)$$

Let us denote by $\mathbf{f}_+$ the total average force per unit area acting on the slab Λ_+ as a whole. This force, directed along the x-axis perpendicular to the plates, is determined by the contact particle densities as follows. The electrolyte localized in the domain Λ_0 contributes to this force by $\beta^{-1}n(d^-/2)\mathbf{e}_x$, where $\mathbf{e}_x$ is the unit vector along the x axis. The Coulomb gas localized in the considered slab Λ_+ contributes by $\beta^{-1}[-n_0(d^+/2) + n_0^{(\mathrm{vac})}]\mathbf{e}_x$, where $n_0^{(\mathrm{vac})}$ is the particle density at $x = d/2 + L$, i.e. the

plain-hard-wall contact density for the Coulomb gas with the bulk density equal to n_0. The resulting force is given by

$$\beta\mathbf{f}_+ = \left\{ n\left(\frac{d^-}{2}\right) - \left[n_0\left(\frac{d^+}{2}\right) - n_0^{(\mathrm{vac})} \right] \right\} \mathbf{e}_x. \tag{3.39}$$

The total force per unit surface acting on the slab Λ_-, $\mathbf{f}_-$, is for symmetry reasons opposite to $\mathbf{f}_+$, $\mathbf{f}_- = -\mathbf{f}_+$. The force $\mathbf{f}$ by which the slab Λ_- acts on the slab Λ_+ is determined as the difference of the force given by (3.39) and its asymptotic $d \to \infty$ separation value,

$$\mathbf{f}(d) = \mathbf{f}_+(d) - \mathbf{f}_+(\infty). \tag{3.40}$$

Equivalently,

$$\beta\mathbf{f} = (\delta n - \delta n_0)\mathbf{e}_x, \tag{3.41}$$

where

$$\delta n = n\left(\frac{d^-}{2}\right) - n\left(\frac{d^-}{2}\right)\Big|_{d\to\infty}, \quad \delta n_0 = n_0\left(\frac{d^+}{2}\right) - n_0\left(\frac{d^+}{2}\right)\Big|_{d\to\infty}. \tag{3.42}$$

After some algebra one gets

$$\beta\mathbf{f}(d) = -\frac{(\kappa_0^2-\kappa^2)^2}{2^{\nu-1}\pi^{(\nu-1)/2}\Gamma\left(\frac{\nu-1}{2}\right)} \int_0^\infty \mathrm{d}l \frac{l^{\nu-2}\sqrt{\kappa^2+l^2}}{\left(\sqrt{\kappa_0^2+l^2}+\sqrt{\kappa^2+l^2}\right)^2} \times \frac{1}{W(l)} \exp\left(-\sqrt{\kappa^2+l^2}d\right) \mathbf{e}_x. \tag{3.43}$$

$W(l)$ is defined by (3.37). Note that the force between the slabs is always attractive. The large-distance asymptotic of this force depends on whether $\kappa = 0$ or $\kappa > 0$.

When there is vacuum between the slabs, i.e. $\kappa \equiv 0$, rescaling l into $l = \kappa_0 k$, the amplitude f of the attractive force can be expressed as

$$\beta f = \frac{\kappa_0^\nu}{2^{\nu-1}\pi^{(\nu-1)/2}\Gamma\left(\frac{\nu-1}{2}\right)} \int_0^\infty \frac{\mathrm{d}k\, k^{\nu-1}}{\left(\sqrt{1+k^2}+k\right)^2} \exp\left(-k\kappa_0 d\right) \times \left\{ \left(\sqrt{1+k^2}+k\right)^2 \sinh(k\kappa_0 d) + 2k\sqrt{1+k^2}\exp(-k\kappa_0 d) \right\}^{-1}. \tag{3.44}$$

In the large-distance limit $\kappa_0 d \to \infty$, one introduces the new integration variable $k' \in \langle 0, \infty)$ via $k = k'/(\kappa_0 d)$, and then expands the integrated function in $1/(\kappa_0 d)$, with the result

$$\beta f = \frac{1}{d^\nu} \frac{(\nu-1)\Gamma(\nu/2)\zeta(\nu)}{2^\nu \pi^{\nu/2}} \left\{ 1 - \frac{2\nu}{\kappa_0 d} + O\left(\frac{1}{(\kappa_0 d)^2}\right) \right\}. \tag{3.45}$$

The first term on the rhs of equation (3.45) corresponds to the electrostatic Casimir force in the ideal-conductor limit of the walls, the second term describes the leading (still long-ranged) non-ideality correction due to the finite correlation length $1/\kappa_0$ of the Coulomb gas forming the slabs. In the short-distance limit $\kappa_0 d \to 0$, one finds from (3.44) that

$$\beta f = \frac{\kappa_0^\nu}{2^\nu \pi^{(\nu-1)/2}\Gamma\left(\frac{\nu-1}{2}\right)} \int_0^\infty \frac{\mathrm{d}k\, k^{\nu-2}}{\sqrt{1+k^2}} \frac{1}{\left(\sqrt{1+k^2}+k\right)^2}. \tag{3.46}$$

Explicitly,

$$\beta f = \begin{cases} \kappa_0^2/(8\pi), & (\nu = 2), \\ \kappa_0^3/(24\pi), & (\nu = 3). \end{cases} \tag{3.47}$$

In the short-distance limit, the density of particles at $x = d^+/2$ is in fact the bulk density n_0, so that $\beta f = n_0 - n_0^{(\mathrm{vac})}$. According to [20], $n_0^{(\mathrm{vac})} = n_0 - \kappa_0^2/(8\pi)$ in 2D and $n_0^{(\mathrm{vac})} = n_0 - \kappa_0^3/(24\pi)$ in 3D, which confirms the obtained results (3.47).

When there is an electrolyte between the slabs, i.e. $\kappa > 0$, the amplitude f of the attractive force between the slabs, see equation (3.43), can be expressed in the large-separation limit $d \to \infty$ as follows

$$\beta f \underset{d\to\infty}{\sim} \frac{2(\kappa_0^2 - \kappa^2)^2}{(4\pi)^{(\nu-1)/2}\Gamma\left(\frac{\nu-1}{2}\right)} \int_0^\infty \frac{\mathrm{d}l\, l^{\nu-2}\sqrt{\kappa^2 + l^2}}{\left(\sqrt{\kappa_0^2 + l^2} + \sqrt{\kappa^2 + l^2}\right)^4} \exp\left(-2\sqrt{\kappa^2 + l^2}d\right). \tag{3.48}$$

Introducing the new integration variable $k \in \langle 0, \infty)$ via $\sqrt{\kappa^2 + l^2} = \kappa + k/d$ and then taking the limit $\kappa d \to \infty$, one finds the exponentially decaying force

$$\beta f \underset{d\to\infty}{\sim} \frac{(\kappa_0 - \kappa)^2}{(\kappa_0 + \kappa)^2} \frac{\kappa^\nu}{(4\pi\kappa d)^{(\nu-1)/2}} \exp(-2\kappa d). \tag{3.49}$$

If the slabs are made from ideal conductors ($\kappa_0 \to \infty$) or they are empty ($\kappa_0 = 0$, i.e. plain hard walls with $\epsilon = 1$) this short-distance force takes the form

$$\beta f \underset{d\to\infty}{\sim} \frac{\kappa^\nu}{(4\pi\kappa d)^{(\nu-1)/2}} \exp(-2\kappa d). \tag{3.50}$$

Note that the parameter (2κ) in the exponential decay corresponds to the inverse correlation length of the density-density distribution functions in the Debye-Hückel limit [34]. We conclude that the presence of an electrolyte between the conducting slabs induces screening of the long-ranged Casimir force.

3.4. Plasma between dielectric walls

We consider the case of a Coulomb gas between dielectric walls. We do not use any microscopic description of the walls and resort to the phenomenological separation (2.9). The derivative $\partial F_0/\partial d$ where F_0 is the free energy of the wall system alone has already been calculated in section 2.2. We now use the Debye-Hückel theory for computing the derivative $\partial\Omega_{\mathrm{eff}}/\partial d$ where Ω_{eff} is the grand potential of the Coulomb gas computed with the Hamiltonian H_{eff}, i.e. with inert dielectric walls. The geometry is the same as in section 2.2, except that now a Coulomb gas with the Debye inverse length κ fills the slab $-d/2 < x < d/2$.

We shall use (3.14), thus we need the screened potential G. Let the source point $\mathbf{r}_2 = (x_2, \mathbf{r}_2^\perp)$ be in the Coulomb gas. The Fourier transform $\hat{G}$ of the screened potential is determined by the equations

$$\left(\frac{\partial^2}{\partial x_1^2} - \kappa^2 - l^2\right) \hat{G}(x_1, x_2; \mathbf{l}) = -s_\nu \delta(x_1 - x_2), \qquad (-d/2 < x_1 < d/2), \tag{3.51a}$$

$$\left(\frac{\partial^2}{\partial x_1^2} - l^2\right) \hat{G}(x_1, x_2; \mathbf{l}) = 0, \qquad (x_1 < -d/2 \text{ or } x_1 > d/2), \tag{3.51b}$$

with the conditions that $\hat{G}$ and $\epsilon(\partial\hat{G}/\partial x_1)$ (with $\epsilon = 1$ in the plasma region) be continuous at $x_1 = \pm d/2$ and that $\hat{G} \to 0$ when $x_1 \to \pm\infty$. A derivation similar to the one in the previous section 3.3 gives, when both x_1 and x_2 are in the Coulomb gas,

$$\hat{G}(x_1,x_2;\mathbf{l}) = \frac{s_\nu}{\sqrt{\kappa^2+l^2}}\left\{\frac{1}{2}\exp\left(-\sqrt{\kappa^2+l^2}|x_1-x_2|\right)\right.$$
$$\left.+\frac{b_l\cosh\left[\sqrt{\kappa^2+l^2}(x_1+x_2)\right]+b_l^2\exp\left(-\sqrt{\kappa^2+l^2}d\right)\cosh\left[\sqrt{\kappa^2+l^2}(x_1-x_2)\right]}{\exp\left(\sqrt{\kappa^2+l^2}d\right)-b_l^2\exp\left(-\sqrt{\kappa^2+l^2}d\right)}\right\} \quad (3.52)$$

where

$$b_l = \frac{\sqrt{\kappa^2+l^2}-\epsilon l}{\sqrt{\kappa^2+l^2}+\epsilon l}. \quad (3.53)$$

We now use (3.52) in (3.14). The first term in the curly brackets of (3.52) corresponds to the bulk G; using the bulk relation (3.5) and linearizing the exponential in (3.14) gives

$$n(x)-n = -\frac{\beta n}{2}\int\frac{\mathrm{d}^{\nu-1}l}{(2\pi)^{\nu-1}}\frac{s_\nu}{\sqrt{\kappa^2+l^2}}\frac{b_l\cosh\left(2\sqrt{\kappa^2+l^2}x\right)+b_l^2\exp\left(-\sqrt{\kappa^2+l^2}d\right)}{\exp\left(\sqrt{\kappa^2+l^2}d\right)-b_l^2\exp\left(-\sqrt{\kappa^2+l^2}d\right)}. \quad (3.54)$$

Therefore

$$\int_{-d/2}^{d/2}\mathrm{d}x[n(x)-n] = -\frac{\beta n}{2}\int\frac{\mathrm{d}^{\nu-1}l}{(2\pi)^{\nu-1}}\frac{s_\nu}{\kappa^2+l^2}$$
$$\times\frac{b_l\sinh\left(\sqrt{\kappa^2+l^2}d\right)+b_l^2\sqrt{\kappa^2+l^2}d\exp\left(-\sqrt{\kappa^2+l^2}d\right)}{\exp\left(\sqrt{\kappa^2+l^2}d\right)-b_l^2\exp\left(-\sqrt{\kappa^2+l^2}d\right)}. \quad (3.55)$$

The grand potential Ω_{eff} is the sum of a bulk part and a surface part (due to the walls) Ω_W. This surface part is related to the surface part of the number of particles (3.55) by

$$n\frac{\partial(-\beta\Omega_W)}{\partial n} = \mathcal{A}\int_{-d/2}^{d/2}\mathrm{d}x[n(x)-n] \quad (3.56)$$

since, at the lowest order in β, we can replace $z\partial/\partial z$ by $n\partial/\partial n$.

In the limit $d\to\infty$, $\Omega_W/\mathcal{A}$ reduces to twice the surface tension γ, and (3.56) with the limiting form of (3.55) give

$$n\frac{\partial(\beta\gamma)}{\partial n} = \frac{\kappa^2}{8}\int\frac{\mathrm{d}^{\nu-1}l}{(2\pi)^{\nu-1}}\frac{b_l}{\kappa^2+l^2}. \quad (3.57)$$

The rescaling of l into $l=\kappa k$ makes apparent that the r.h.s. of (3.57) depends on n by a factor $\kappa^{\nu-1}$. Using $n\partial/\partial n = (1/2)\kappa\partial/\partial\kappa$, we can integrate (3.57) into

$$\beta\gamma = \frac{\kappa^{\nu-1}}{4(\nu-1)}\int\frac{\mathrm{d}^{\nu-1}k}{(2\pi)^{\nu-1}}\frac{1}{1+k^2}\frac{\sqrt{1+k^2}-\epsilon k}{\sqrt{1+k^2}+\epsilon k}. \quad (3.58)$$

In 2D, performing the integral in (3.58) gives

$$\beta\gamma = \begin{cases} \dfrac{\kappa}{2\pi}\left[-\dfrac{\pi}{4} + \dfrac{2}{\sqrt{1-\epsilon^2}}\tan^{-1}\left(\dfrac{1-\epsilon}{1+\epsilon}\right)^{1/2}\right] & \text{if } \epsilon < 1, \\ \dfrac{\kappa}{2\pi}\left[-\dfrac{\pi}{4} + \dfrac{2}{\sqrt{\epsilon^2-1}}\tanh^{-1}\left(\dfrac{\epsilon-1}{\epsilon+1}\right)^{1/2}\right] & \text{if } \epsilon > 1. \end{cases} \tag{3.59}$$

In 3D, for $\epsilon = 1$, (3.58) reproduces the $\nu = 3$ surface tension (3.27). For other values of ϵ, the integral in (3.58) diverges. When $\epsilon > 1$, this divergence is to be expected for point particles, since the interaction between a particle and its image is attractive and produces a non-integrable Boltzmann factor. However, when $\epsilon < 1$, the divergence comes from the inappropriate linearization of the exponential in (3.14); a more careful treatment [35, 13] gives a finite surface tension.

For a finite distance d, the d-dependent part of the grand potential per unit area is $\omega_{\text{eff}}(d) = (\Omega_W/\mathcal{A}) - 2\gamma$. After the substraction of the infinite-d part of (3.55), using again $n\partial/\partial n = (1/2)\kappa\partial/\partial\kappa$, we now obtain

$$\frac{\partial(\beta\omega_{\text{eff}})}{\partial\kappa} = \frac{1}{2(2\pi)^{\nu-1}}\int \mathrm{d}^{\nu-1}l \times \frac{\kappa[b_l(b_l^2-1)(\kappa^2+l^2)^{-1} + 2b_l^2 d(\kappa^2+l^2)^{-1/2}]\exp(-2d\sqrt{\kappa^2+l^2})}{1-b_l^2\exp(-2d\sqrt{\kappa^2+l^2})}. \tag{3.60}$$

It can be checked that the numerator in the integrand of (3.60) is the derivative with respect to κ of the denominator. Thus, integrating (3.60) with the condition $\omega_{\text{eff}} = 0$ when $\kappa = 0$ gives

$$\beta\omega_{\text{eff}} = \frac{1}{2(2\pi)^{\nu-1}}\int \mathrm{d}^{\nu-1}l \left\{ \ln\left[1-b_l^2\exp(-2d\sqrt{\kappa^2+l^2})\right] - \ln\left[1-\left(\frac{1-\epsilon}{1+\epsilon}\right)^2\exp(-2dl)\right]\right\}. \tag{3.61}$$

The second logarithm in equation (3.61) gives to the force $-\partial\omega_{\text{eff}}/\partial d$ a long-range contribution opposite to the Casimir force in vacuum (2.15): the total long-range force associated to $\omega = \omega_{\text{eff}} + (F_0/\mathcal{A})$ vanishes. The cancellation (screening) effect does occur in the present model. Only a short-range d-dependent force remains, associated to

$$\beta\omega = \frac{1}{2(2\pi)^{\nu-1}}\int \mathrm{d}^{\nu-1}l\, \ln\left[1-b_l^2\exp(-2d\sqrt{\kappa^2+l^2}\,)\right]. \tag{3.62}$$

Thus, in the 3D case $\nu = 3$, we have retrieved by our method a previously known result [36, 13].

In the limit $\kappa d \to \infty$, the asymptotic behaviour of (3.62) is

$$\beta\omega \sim -\frac{1}{2(2\pi)^{\nu-1}}\int \mathrm{d}^{\nu-1}l\, b_l^2\exp(-2d\sqrt{\kappa^2+l^2}). \tag{3.63}$$

In this equation, only small values of l/κ contribute to the integral. Thence, $\exp(-2d\sqrt{\kappa^2+l^2}) \sim \exp(-2\kappa d - dl^2/\kappa)$ and $b_l^2 \sim 1$. With these replacements in (3.63),

$$\beta\omega \sim -\frac{\kappa^{(\nu-1)/2}\exp(-2\kappa d)}{2^\nu(\pi d)^{(\nu-1)/2}}, \tag{3.64}$$

and the force per unit area has the asymptotic behaviour for large κd

$$-\frac{\partial \omega}{\partial d} \sim -\frac{\beta^{-1}\kappa^{\nu}\exp(-2\kappa d)}{(4\pi\kappa d)^{(\nu-1)/2}}. \tag{3.65}$$

This asymptotic behaviour has the remarkable feature that it does not depend on ϵ. This was already apparent on (3.49) in the special cases $\epsilon = 1$ ($\kappa_0 = 0$) and $\epsilon \to \infty$ ($\kappa_0 \to \infty$).

4. The free-fermion point

4.1. General formalism

The 2D symmetric Coulomb gas is exactly solvable at the collapse coupling $\beta = 2$ by mapping onto the Thirring model at the free fermion point. We first shortly review the bulk regime. Both species of particles have the same rescaled fugacity $m = 2\pi a z$ [where a is the length scale introduced in equation (1.2)] which has the dimension of an inverse length. The general formalism [17, 24] expresses the many-particle densities in terms of specific Green functions $G_{qq'}(\mathbf{r}, \mathbf{r}')$ ($q, q' = \pm$). Because of the symmetry between positive and negative particles, one only needs G_{++} and G_{-+} which are determined by

$$(\Delta_1 - m^2) G_{++}(\mathbf{r}_1, \mathbf{r}_2) = -m\delta(\mathbf{r}_1 - \mathbf{r}_2) \tag{4.1}$$

and

$$G_{-+}(\mathbf{r}_1, \mathbf{r}_2) = -\frac{1}{m}\left(\frac{\partial}{\partial x_1} + \mathrm{i}\frac{\partial}{\partial y_1}\right) G_{++}(\mathbf{r}_1, \mathbf{r}_2). \tag{4.2}$$

These equations have to be supplemented by the vanishing boundary conditions when $|\mathbf{r}_1 - \mathbf{r}_2| \to \infty$. In infinite space, the solution of equations (4.1) and (4.2) reads

$$G_{++}(\mathbf{r}_1, \mathbf{r}_2) = \frac{m}{2\pi} K_0(m|\mathbf{r}_1 - \mathbf{r}_2|), \tag{4.3a}$$

$$G_{-+}(\mathbf{r}_1, \mathbf{r}_2) = \frac{m}{2\pi} \frac{(x_1 - x_2) + \mathrm{i}(y_1 - y_2)}{|\mathbf{r}_1 - \mathbf{r}_2|} K_1(m|\mathbf{r}_1 - \mathbf{r}_2|), \tag{4.3b}$$

where K_0 and K_1 are modified Bessel functions. The one-particle densities, given by

$$n_q = m G_{qq}(\mathbf{r}, \mathbf{r}), \tag{4.4}$$

are infinite since $K_0(mr)$ diverges logarithmically as $r \to 0$. This divergence can be suppressed by a short-distance cutoff R. We replace the point-like particles by small charged hard disks of diameter R and use a regularized form of (4.4) for the total particle density $n = n_+ + n_-$,

$$n = \frac{m^2}{\pi} K_0(mR) \underset{mR \to 0}{\sim} \frac{m^2}{\pi}\left[\ln\left(\frac{2}{mR}\right) - C\right]. \tag{4.5}$$

Such a regularization is consistent in the sense that the perfect-screening sum rule is satisfied and the expected equation of state is reproduced [17, 24].

The above formalism can be generalized to inhomogeneous situations when the system domain $\Lambda = \cup_\alpha \Lambda^{(\alpha)}$. Each subdomain $\Lambda^{(\alpha)}$ is characterized by a constant rescaled

fugacity, $m(\mathbf{r}) = m_\alpha$ for $\mathbf{r} \in \Lambda^{(\alpha)}$, and the corresponding bulk density n_α defined as a function of m_α by (4.5). The Green function G_{++} obeys the differential equation

$$(\Delta_1 - m_\alpha^2) G_{++}(\mathbf{r}_1, \mathbf{r}_2) = -m_\alpha \delta(\mathbf{r}_1 - \mathbf{r}_2), \qquad \mathbf{r}_1 \in \Lambda^{(\alpha)}, \tag{4.6}$$

where the spatial position of the source point $\mathbf{r}_2$ is arbitrary. The Green function G_{-+} is determined by G_{++} via equation (4.2) with m taken as the subdomain-dependent $m(\mathbf{r}_1)$. The boundary conditions are that G_{++} and G_{-+} must be continuous at each subdomain boundary $\partial\Lambda^{(\alpha)}$. The one-particle densities are again given by (4.4).

4.2. Polarizable interface

In the geometry of figure 1, the rescaled particle fugacity is equal to m in the half-space $x > 0$ and to m_0 in the half-space $x < 0$. Let the source point $\mathbf{r}_2 = (x_2, y_2)$ has the coordinate $x_2 > 0$. In the Fourier representation (3.15), equation (4.6) takes the form

$$\left(\frac{\partial^2}{\partial x_1^2} - m^2 - l^2\right) \hat{G}_{++}(x_1, x_2; l) = -m\delta(x_1 - x_2), \qquad (x_1 > 0), \tag{4.7a}$$

$$\left(\frac{\partial^2}{\partial x_1^2} - m_0^2 - l^2\right) \hat{G}_{++}(x_1, x_2; l) = 0, \qquad (x_1 < 0). \tag{4.7b}$$

We look for a solution, vanishing at $x_1 \to \pm\infty$, of the form

$$\hat{G}_{++} = \frac{m}{2\sqrt{m^2 + l^2}} \exp\left(-\sqrt{m^2 + l^2}|x_1 - x_2|\right) + A_l \exp\left[-\sqrt{m^2 + l^2}(x_1 + x_2)\right], \qquad (x_1 > 0), \tag{4.8a}$$

$$\hat{G}_{++} = B_l \exp\left(\sqrt{m_0^2 + l^2}x_1 - \sqrt{m^2 + l^2}x_2\right), \qquad (x_1 < 0). \tag{4.8b}$$

The constants A_l and B_l are determined by the conditions that $\hat{G}_{++}$ and $\hat{G}_{-+} = [m(x_1)]^{-1}(l - \partial_{x_1})\hat{G}_{++}$ are continuous at $x_1 = 0$. The final result is

$$A_l = -\frac{m}{2\sqrt{m^2 + l^2}} + B_l, \tag{4.9a}$$

$$B_l = \left(\frac{\sqrt{m^2 + l^2} + l}{m} + \frac{\sqrt{m_0^2 + l^2} - l}{m_0}\right)^{-1}. \tag{4.9b}$$

The particle density at $x > 0$ is then given by

$$n(x) = n + \frac{m}{\pi} \int_0^\infty \mathrm{d}l \, (A_l + A_{-l}) \exp\left(-2\sqrt{m^2 + l^2}x\right), \tag{4.10}$$

where n is the regularized bulk density related to the rescaled fugacity m via (4.5). The same procedure applies when the source point $\mathbf{r}_2 = (x_2, y_2)$ has the component $x_2 < 0$. For symmetry reasons, one gets the particle density at $x < 0$ in the form $n_0(x) = n_0 +$the last term of equation (4.10) with the interchange $m \leftrightarrow m_0$.

The surface tension γ is again determined by the relations

$$m\frac{\partial(-\beta\gamma)}{\partial m} = \int_0^\infty \mathrm{d}x \, [n(x) - n], \tag{4.11a}$$

$$m_0\frac{\partial(-\beta\gamma)}{\partial m_0} = \int_{-\infty}^0 \mathrm{d}x \, [n_0(x) - n_0], \tag{4.11b}$$

with the boundary condition $\beta\gamma(m, m_0) = 0$ when $m = m_0$. The result is

$$\beta\gamma = \int_0^\infty \frac{\mathrm{d}l}{2\pi} \ln\left(\frac{2\sqrt{m^2+l^2}\sqrt{m_0^2+l^2}}{mm_0+\sqrt{m^2+l^2}\sqrt{m_0^2+l^2}+l^2}\right). \tag{4.12}$$

When there are no particles in the half-space $x < 0$, i.e. $m_0 = 0$, (4.12) yields the surface tension of the Coulomb gas in contact with a vacuum,

$$\beta\gamma^{(\mathrm{vac})}(m) = \frac{m}{4\pi}(\pi - 2), \tag{4.13}$$

in full agreement with the result obtained in [17].

In the ideal-conductor limit of the Coulomb gas in the half-space $x < 0$, the surface tension of equation (4.12) has the following large-m_0 expansion

$$\beta\gamma = \frac{m_0}{4\pi}(\pi - 2) + m\left[\frac{1}{2\pi}\ln\left(\frac{m}{m_0}\right) + O(1)\right]. \tag{4.14}$$

The first term on the rhs of equation (4.14) is nothing but the vacuum surface tension [see (4.13)] of the Coulomb gas in the half-space $x < 0$. The second term, the surface tension of the Coulomb gas at $x > 0$ induced by the ideal-conductor wall at $x < 0$, diverges due to the particle-image collapse at $\beta = 2$ [28].

4.3. Two-slab geometry

The above method can be readily extended to the two-slab geometry of figure 2. We keep the notation of intervals $X_+ = \langle d/2, \infty)$, $X_0 = \langle -d/2, d/2\rangle$ and $X_- = (-\infty, -d/2\rangle$ from section 3.3. If the source point $\mathbf{r}_2 = (x_2, y_2)$ has the coordinate $x_2 \in X_+$, the solution of equations (4.6) is searched, in the Fourier space, in the form

$$\hat{G}_{++} = \frac{m_0}{2\sqrt{m_0^2+l^2}} \exp\left(-\sqrt{m_0^2+l^2}|x_1 - x_2|\right) + A_l \exp\left[-\sqrt{m_0^2+l^2}(x_1+x_2)\right], \qquad (x_1 \in X_+), \tag{4.15a}$$

$$\hat{G}_{++} = \exp\left(-\sqrt{m_0^2+l^2}x_2\right)\left[B_l \exp\left(\sqrt{m^2+l^2}x_1\right) + C_l \exp\left(-\sqrt{m^2+l^2}x_1\right)\right], \qquad (x_1 \in X_0), \tag{4.15b}$$

$$\hat{G}_{++} = D_l \exp\left[\sqrt{m_0^2+l^2}(x_1 - x_2)\right], \qquad (x_1 \in X_-). \tag{4.15c}$$

The unknown constants A_l, B_l, C_l and D_l are determined by the conditions that $\hat{G}_{++}$ and $[m(x_1)]^{-1}(l - \partial_{x_1})\hat{G}_{++}$ are continuous at $x_1 = \pm d/2$. The particle density at $x \geq d/2$ is determined by

$$n_0(x) = n_0 + \frac{m_0}{\pi}\int_0^\infty \mathrm{d}l\,(A_l + A_{-l}) \exp\left(-2\sqrt{m_0^2+l^2}x\right). \tag{4.16}$$

The same formalism applies when the source point $\mathbf{r}_2 = (x_2, y_2)$ has the coordinate $x_2 \in X_0$, to obtain the density profile between the slabs.

The force between the slabs is calculated by using the procedure outlined in section 3.3, formulae (3.39) - (3.43). Without going into technical details, we have found that

the force $\mathbf{f}(d)$, defined by (3.40), is always attractive. Its amplitude f as a function of the distance d between the slabs is given by

$$\beta f(d) = \frac{(m_0-m)^2}{\pi}\int_0^\infty \mathrm{d}l \frac{l^2\sqrt{m^2+l^2}}{mm_0+\sqrt{m^2+l^2}\sqrt{m_0^2+l^2}+l^2} \times \frac{1}{W(l)}\exp\left(-\sqrt{m^2+l^2}d\right), \tag{4.17a}$$

where

$$W(l) = \left(mm_0+\sqrt{m^2+l^2}\sqrt{m_0^2+l^2}+l^2\right)\sinh\left(\sqrt{m^2+l^2}d\right) + \sqrt{m^2+l^2}\sqrt{m_0^2+l^2}\exp\left(-\sqrt{m^2+l^2}d\right). \tag{4.17b}$$

The large-distance behaviour of $f(d)$ depends on whether the rescaled fugacity $m = 0$ or $m > 0$.

When there is vacuum between the slabs, i.e. $m \equiv 0$, the amplitude of the attractive force can be expressed in the limit $m_0 d \to \infty$ as follows

$$\beta f = \frac{\pi}{24d^2}\left\{1 - \frac{4}{(2m_0)d} + O\left(\frac{1}{(m_0 d)^2}\right)\right\}. \tag{4.18}$$

The first term on the rhs of equation (4.18) corresponds to the 2D electrostatic Casimir force in the ideal-conductor limit of the slabs, the second term corresponds to the correction due to the finite correlation length $1/(2m_0)$ of the Coulomb gas forming the slabs. It is interesting that this correction, evaluated at the $\beta = 2$ collapse point, has the same form (in terms of the correlation length) as the one evaluated in the Debye-Hückel $\beta \to 0$ limit, see formula (3.45).

When there is an electrolyte between the slabs, i.e. $m > 0$, the amplitude of the attractive force has the following large-d behaviour

$$\beta f \underset{d\to\infty}{\sim} \begin{cases} \dfrac{(m_0-m)^2}{m_0^2}\dfrac{m^2}{8\sqrt{\pi}(md)^{3/2}}\exp(-2md) & \text{for } m_0 > 0, \\ \dfrac{m^2}{\sqrt{\pi md}}\exp(-2md) & \text{for } m_0 = 0\ . \end{cases} \tag{4.19}$$

If the slabs are made from an ideal-conductor material with $m_0 \to \infty$, this short-distance force is written as

$$\beta f \underset{d\to\infty}{\sim} \frac{m^2}{8\sqrt{\pi}(md)^{3/2}}\exp(-2md). \tag{4.20}$$

These formulae confirm that, also at the special $\beta = 2$ coupling, an electrolyte between the ideal-conductor slabs causes screening of the long-range Casimir force. Comparing with the Debye-Hückel result [see equations (3.49) and (3.50)] one sees that the residual short-range force is temperature-dependent. Note that at $\beta = 2$ the residual force depends on the dielectric constant ϵ of the slabs, since the results (4.19) for $\epsilon = 1$ ($m_0 = 0$) and (4.20) for $\epsilon \to \infty$ are different. The non-dependence on ϵ found in (3.50) and (3.65) seems to hold only in the Debye-Hückel regime.

5. Conclusion

On fully microscopic models, in the classical (i.e. non quantum) regime, we have studied the properties of a Coulomb gas near a plane conducting wall, and two parallel conducting walls with or without a Coulomb gas between them. We have also considered the case of dielectric walls of arbitrary dielectric constant ϵ, without a microscopic model for these walls, using macroscopic electrostatics and linear response theory. We have checked that the long-range Casimir force between parallel walls separated by a vacuum is screened into some (still attractive) residual short-range force when a Coulomb gas is present between the walls.

All these calculations have been performed taking into account only the electrostatic part of the interactions. How to take into account the magnetic field for dealing, on a microscopic model in the classical limit, with the full particle-radiation interaction is an open problem.

Acknowledgments

The authors acknowledge support from the CNRS-SAS agreement, Project No. 14439. A partial support of L. Šamaj by a VEGA grant is acknowledged.

References

[1] Duplantier B, 2003 *Poincaré Seminar 2002* ed B Duplantier and V Rivasseau (Basel: Birkhäuser) p 53
[2] Bordag M, Mohideen U and Mostepanko V M, 2001 *Phys. Rep.* **353** 1
[3] Lifshitz E M, 1954 *Sov. Phys. JETP* **2** 73
Dzyaloshinskii I E, Lifshitz E M and Pitaevskii L P, 1961 *Sov. Phys. Uspekhi* **73** 381
[4] Schwinger J, DeRaad L L and Milton K A, 1978 *Ann. Phys.* **115** 1
[5] Balian R and Duplantier B, 1977 *Ann. Phys.* **104** 300
Balian R and Duplantier B, 1978 *Ann. Phys.* **112** 165
[6] Balian R, 2003 *Poincaré Seminar 2002* ed B Duplantier and V Rivasseau (Basel: Birkhäuser) p 71
[7] Feinberg J, Mann A and Revzen M, 2001 *Ann. Phys.* **288** 103
[8] Mohideen U and Roy A, 1998 *Phys. Rev. Lett.* **81** 4549
[9] Attard P, Mitchell D J and Ninham B W, 1988 *J. Chem. Phys.* **88** 4987
Attard P, Mitchell D J and Ninham B W, 1988 *J. Chem. Phys.* **89** 4358
[10] Téllez G, 2004 *Preprint* cond-mat/0401475, to be published in *Phys. Rev.* E
[11] Jancovici B and Téllez G, 1996 *J. Stat. Phys.* **82** 609
[12] Jancovici B and Šamaj L, 2001 *J. Stat. Phys.* **104** 753
[13] Dean D S and Horgan R R, 2002 *Phys. Rev.* E **65** 061603
Dean D S and Horgan R R, 2003 *Phys. Rev.* E **68** 051104
Dean D S and Horgan R R, 2003 *Phys. Rev.* E **68** 061106
[14] Forrester P J, Jancovici B and Téllez G, 1996 *J. Stat. Phys.* **84** 359
[15] Jancovici B and Téllez G, 1996 *J. Phys. A: Math. Gen.* **29** 1155
[16] Buenzli P R and Martin Ph A, 2004 *Preprint: Microscopic origin of universality in Casimir forces*, Institute of Theoretical Physics, Swiss Federal Institute of Technology, Lausanne (June 2004)
[17] Cornu F and Jancovici B, 1989 *J. Chem. Phys.* **90** 2444
[18] Forrester P J, 1990 *J. Chem. Phys.* **95** 4545

Forrester P J, 1992 *J. Stat. Phys.* **67** 433
[19] Martin Ph A, 1988 *Rev. Mod. Phys.* **60** 1075
[20] Jancovici B, 1982 *J. Stat. Phys.* **28** 43
[21] Choquard Ph, Piller B, Rentsch R and Vieillefosse P, 1989 *J. Stat. Phys.* **55** 1185
[22] Kalinay P, Markoš P, Šamaj L and Travěnec I, 2000 *J. Stat. Phys.* **98** 639
[23] Jancovici B, Kalinay P and Šamaj L, 2000 *Physica* A **279** 260
[24] Cornu F and Jancovici B, 1987 *J. Stat. Phys.* **49** 33
[25] Zamolodchikov Al B, 1995 *Int. J. Mod. Phys.* A **10** 1125
[26] Bajnok Z, Palla L and Takács G, 2002 *Nucl. Phys.* B **622** 565
[27] Šamaj L and Travěnec I, 2000 *J. Stat. Phys.* **101** 713
[28] Šamaj L and Jancovici B, 2001 *J. Stat. Phys.* **103** 717
[29] Šamaj L, 2001 *J. Stat. Phys.* **103** 737
[30] Jancovici B, 1995 *J. Stat. Phys.* **80** 445
[31] Jackson J D, 1975 *Classical Electrodynamics* 2nd edn. (New York: John Wiley)
[32] Gradshteyn I S and Ryzhik I M, 1994 *Table of Integrals, Series and Products* 5th edn. (London: Academic Press)
[33] Russier V, Badiali J P and Rosinberg M L, 1985 *J. Phys. C: Solid State Phys.* **18** 707
[34] Šamaj L and Jancovici B, 2002 *J. Stat. Phys.* **106** 323
[35] Onsager L and Samaras N T, 1934 *J. Chem. Phys.* **2** 528
[36] Mahanty J and Ninham B W, 1976 *Dispersion Forces* (London: Academic Press)